TEXAS A&M
UNIVERSITY®

ISEN 658 Course Project

By Group 5

Yu-Heng Chien, Ching-Ju Hsiao, Chia-Wei Liu,

Tsung-Cheng Chen

Instructor: Dr. Sarah Wolff

Date: May 10 , 2022

Contents

1. Intridcution

Tensile testing is a common method for characterizing cast materials in industry and research. The tensile test curve reflects the behavior inside the material, showing the effect of load on elongation. A better understanding can be gained if we can explore the response of tensile and compressive loads more. In this project, we used the 2014 tensile test data provided by the professor for research. The theme of this study will be extended to the formula of $\sigma = K\varepsilon^n$ mentioned in ISEN658 class, and we will try to use experimental data to test whether it is consistent with the above formula.

1.1 Material Property

5754 aluminum alloy has the characteristics of medium strength, good corrosion resistance, weldability and easy processing and forming. It is a typical alloy in Al-Mg alloys. In foreign countries, 5754 aluminum alloy sheets with different heat treatment states are the main materials used in the automobile manufacturing industry (car doors, molds, seals) and the canning industry. 5754 aluminum sheet is widely used in welded structures, storage tanks, pressure vessels, ship structures and offshore facilities, transportation tanks, and in occasions requiring excellent processability, excellent corrosion resistance, high fatigue strength, high weldability and moderate static strength. (see in figure 1 and table 1)

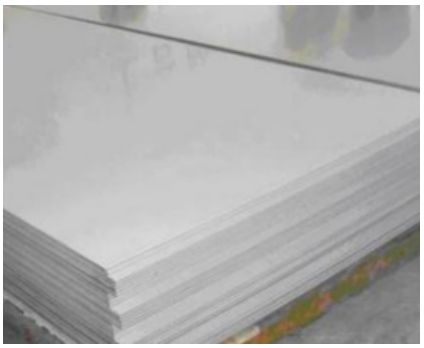

Figure 1

Table 1 Properties of AA 5754 aluminium alloy

Chemical composition %								
Al	Mg	Si	Mn	Zn	Fe	Ti	Cu	Cr
95.73	2.87	0.3	0.05	0.2	0.3	0.2	0.05	0.3

1.2 Data Set

In this part, the data set we used is the experimental data of the tensile test for AA5754-O 1 mm and 2 mm. There are several data type below:

Data type	Description
True Strain	True Strain represents the displacement between particles in the body relative to a reference length.
Yielding stress[Mpa]	The minimum stress at which a solid will undergo permanent deformation or plastic flow without a significant increase in the load or external force.
Tensile stress [Mpa]	Tensile stress measures the strength of a material; It refers to a force that attempts to pull apart or stretch a material.
Uniform elongation	In a tensile test, uniform elongation is the percentage the gauge length elongated at peak load relative to the initial gauge length.
Strength harding component	The strain hardening exponent (also called the strain hardening index), usually denoted n , a constant often used in calculations relating to stress-strain behavior in work hardening.

Additionally, we also have three dimensions of stress for test specimens:

RD refers to Rolling Direction Stress (0°).TDTransverse Direction Stress (90°) and DD Diagonal Direction Stress(45°). Here we use the average stress of these three dimensions. (see in figure 1.2(a) and figure 1.2(b))

2014 Aleris 5ST 1mm

	R value	Yielding Stress	Tensile stress (K)	n_value	uniform elongation	TE	
		MPa	Rm_tech(MPa)	6~12%	Ag_tech(%)	%	
2014-179	0.678	112.17	248.54	0.3	20.06	22.00	
2014-180	0.694	112.46	245.93	0.307	20.83	21.90	90°
2014-181	0.686	112.39	246.08	0.297	18.25	20.70	
2014-183	0.602	109.65	252.74	0.296	18.65	19.50	
2014-184	0.62	110.3	254.19	0.288	17.3	20.80	0°
2014-185	0.611	109.86	249.02	0.302	17.72	19.50	
2014-187	0.81	107.31	242.29	0.305	21.49	23.98	
2014-188	0.814	105.66	238.61	0.304	21.28	22.53	
2014-189	0.802	105.19	240.95	0.303	21.84	23.01	45°
Direction	Averaged data						
90	0.70	109.44	246.48	0.30	19.71	21.55	
0	0.61	109.94	251.98	0.30	17.89	19.93	
45	0.81	106.05	240.62	0.30	21.54	23.17	

figure 1.2 (a)

	R value	Yielding Stress	Tensile stress (K)	n_value	uniform elongation	TE	
		MPa	Rm_tech(MPa)	6~12%	Ag_tech(%)	%	
2014-155	0.724	110.82	240.25	0.323	21.44	24.72	
2014-156	0.71	112.4	241.3	0.321	21.27	25.32	45°
2014-157	0.731	112.19	242.8	0.321	23.73	26.40	
2014-160	0.674	116.79	250.64	0.329	20.5	22.73	0°
2014-161	0.68	115.23	248.57	0.322	18.63	20.10	
2014-162	0.688	114.56	248.01	0.314	17.24	22.59	
2014-163	0.686	114.65	239.5	0.305	26.02	26.76	
2014-164	0.65	112.67	238.31	0.312	21.65	24.75	90°
2014-165	0.675	113.44	237.8	0.303	21.02	23.09	
Direction	Averaged						
45	0.69	111.80	243.02	0.32	21.28	25.48	
0	0.68	115.53	249.07	0.32	18.79	21.81	
90	0.67	113.59	238.54	0.31	22.90	24.87	

figure 1.2(b)

2. Methods

2.1 Manufacturing Process

The process used to acquire this dataset is tensile test. Tensile test is a destructive test method that determines the metallic material's tensile strength, yield strength, and ductility. It decides how much force is necessary to break a composite or plastic specimen, as well as how far the specimen stretches or elongates to reach that breaking point.

The specimens in this project are cut in three directions (RD, TD, DD) in the plane of the sheet. As shown in the following figure, the rolling directionIs RD, the transverse direction as TD, and the direction (45° from the RD) as DD.(see in fig.2.1(a) and (b))

There are three dimensions of test specimens:
(1)Rolling Direction (RD)
(2)Transverse Direction (TD)
(3) Diagonal Direction (DD)

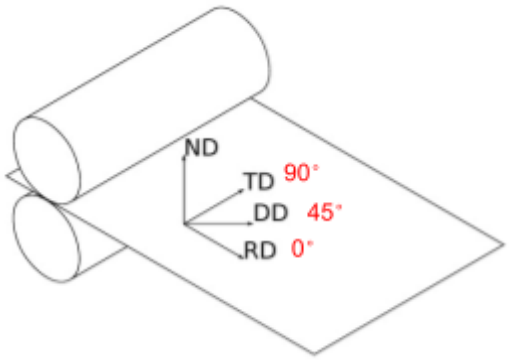

Fig.2.1(a)

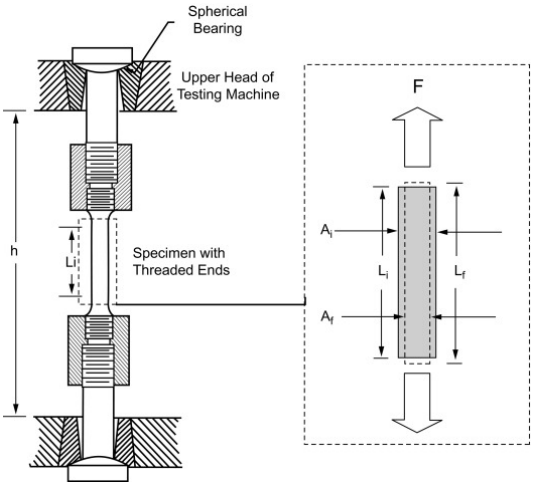

Fig.2.1(b)

The testing speed was set as 1 mm/min and 2 mm/min. There are many parameters we can obtain from performing Tensile test: Young modulus E, yield strength σy, ultimate tensile strength , Lankford coefficients R, strain at the onset of necking ε neck, and fracture strain εf.

The engineering stress is defined as s $\sigma_{eng} = \frac{P}{A_0}$, where P is the instantaneous load during the test and A_0 is

the initial transversal area computed as $w_0 t_0$, where w_0 is the initial width (at the center of the sample) and t_0 is the initial thickness. so $\sigma_{eng} = \frac{P}{A_0}$, where P is the instantaneous load during the test and A0 is the initial transversal area computed as w0t0, where w0 is the initial width (at the center of the sample) and t0 is the initial thickness. Furthermore, the axial engineering strain is defined as $\varepsilon_{eng} = \frac{L-L_0}{L_0}$, where L and L_0 are the current and starting extensometer lengths.

The true stress (which is equal to the equivalent stress for this specific condition), true (logarithmic) strain, and equivalent plastic strain are defined as = eng(1 + eng), = ln(1 + eng), and p = E, respectively, assuming volume invariance and homogeneous stress and strain patterns before necking formation.
To define the material hardening reaction, the equivalent stress in terms of the equivalent plastic strain curve should be employed. The Lankford coefficients, which are defined as Rθ = ε˙w ε˙t , where is the angle with respect to the rolling direction and the real strain rates w and t are connected to the width and thickness evolutions of the sample, are used to quantify the plastic anisotropy. ε˙t = −(ε˙ l + ε˙w), where ε˙ l is the real strain rate in the axial direction of the sample, assuming an isochoric and homogenous plastic flow. True strain rates ε˙w and ε˙ l are determined using the displacement field acquired by DIC at a few particular places along the extensometer length.

2.2 Processing The Data

First, we will organize the Tensile test data and use Python for plotting, modeling, and residual value comparison. Python is one of the widely used computer languages, it can perform calculations and drawings efficiently and quickly. This project will use python to analyze different visual figures. For all figures will plot the experimental data and prediction data on the same plot as well. The accuracy between the models will also be compared using residual analysis, which is commonly used in statistical data analysis, to compare which model has higher accuracy. At last we'll explain why our pick of the best models managed to stand out.

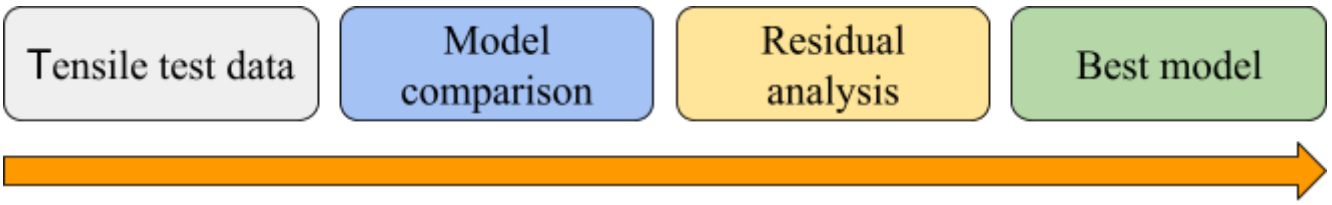

Fig.2.2

From the picture 2.3 is the experimental data of the 1mm and 2mm, uniformly using blue to represent 0 degrees, red to represent 45 degrees, and green to represent 90 degrees. It can be seen in the pictures that there is obvious yield stress, and it can be further found that before the yield stress, the experimental data is almost a straight line, which is in line with the concepts learned in the lecture 2. Conversely, after the yield stress point, all the lines are nonlinear and break when strain is equal to about 25. The mathematical model after the yield stress point is first tested by Ludwik-Hollomon law. Here we use several models in our report:

(1) Ludwik-Hollomon law
(2) Ludwigon Law
(3) Voce constitutive model
(4) Modified Voce hardening model
(5) Swift hardening model
(6) Kim-Tuan constitutive model

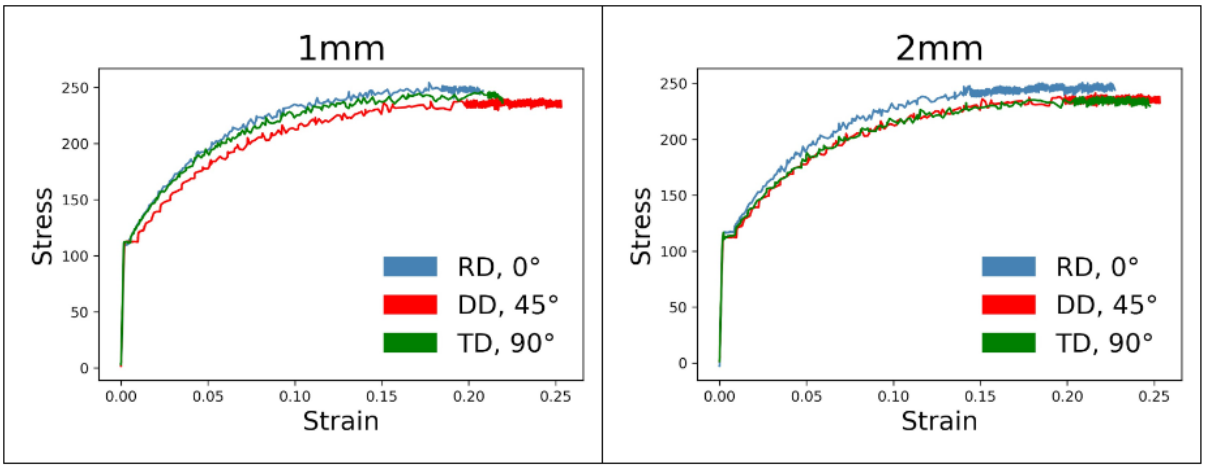

Fig.2.3

3. Results

3.1 Model 1–Ludwik-Hollomon law

An initial method we use unmodified Ludwik-Hollomon relation:

$$\sigma = K\ (\varepsilon\ )^{n} \tag{1.1}$$

Where,

σ is true stress.

ε is true strain.

K is material property constant called "strength coefficient"

n is exponent termed the "strength harding component"

Since the raw data did not conclude K, we use the relation between the ultimate tensile strength (UTS) and strain hardening component. According to *Manufacturing Processes authored by John A. Schey, Third edition, McGraw-Hill ISBN 0-07-03137-4, 2000*, The equation here is given in Schey's book:

$$UTS = K(n/e)^{n} \tag{1.2}$$

Where the e refers to natural logarithm which approximately is 2.7183. Thus, we use this equation to find K respectively in 1 mm and 2 mm.Table 1 and 2 illustrate the related coefficient of AA5754-O material.

Table 2 *Mechanical properties of AA5754-O aluminum alloy of 1mm*

	K	σy[Mpa]	εy[Mpa]	UTS	n
RD (0°)	485.370	109.937	0.000066	251.983	0.300
DD (45°)	468.337	106.053	0.000076	240.617	0.295
TD (90°)	475.802	109.443	0.000080	246.483	0.304

*** E refers to Young's modulas , here we use E = 68 Gpa**

Table 3 *Mechanical properties of AA5754-O aluminum alloy of 2mm*

	K	σy[Mpa]	εy[Mpa]	UTS	n
RD (0°)	492.900	115.527	0.000109	249.073	0.321
DD (45°)	482.800	111.803	0.000106	243.020	0.322
TD (90°)	473.920	113.587	0.000118	238.537	0.307

*** E refers to Young's modulas , here we use E = 68 Gpa**

Also after calculating the true stress and strain, we transfer to engineering strain and stress by equation:

$$\sigma_t = \sigma_e(1 + \varepsilon_e) \quad (1.3)$$

$$\varepsilon_t = ln(1 + \varepsilon_e) \quad (1.4)$$

Figure 2.4 is a comparison between the prediction results using the Ludwik-Hollomon law and the experimental data. We add the 1 mm and 2 mm prediction data for comparison. The data of 1 mm and 2 mm have some similarities. For example, the stress data of DD is smaller than that of RD and TD. There is a considerable gap between 1 mm and 2 mm even though that gap is not seen as an obvious difference if we look at the gap between prediction and experimental data.

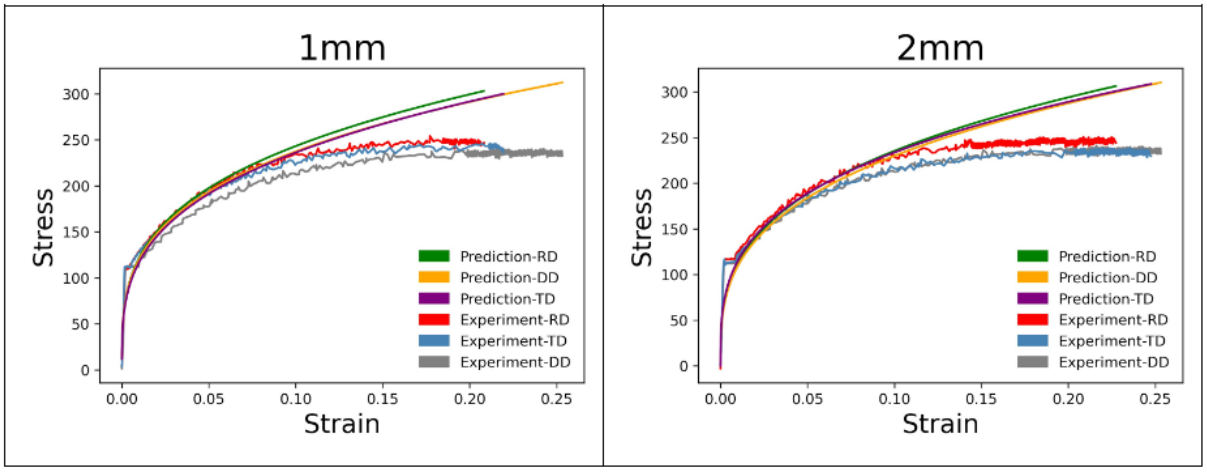

Figure 2.4

By matching the experimental data, it can be found that there is still a significant difference between the experimental data and the prediction data based on the Hollomon equation. Taking the left side of the figure as an example, the three angles RD, DD, and TD are represented by green, orange, and purple lines, respectively. After strain is equal to 15, three lines are at least 800 or more different from the experimental group of data. The right and left figures show a huge difference with the experimental data.

With the residual plot, the gap between the predicted numbers and the experimental numbers can be seen more clearly by being used as a quantitative indicator for this group. The right picture of Figure 2.5 shows the difference between the predicted value and the actual value with strain as the x-axis. Using the Ludwik-Hollomon law, there is a huge residual in this tensile experiment prediction, and it tends to

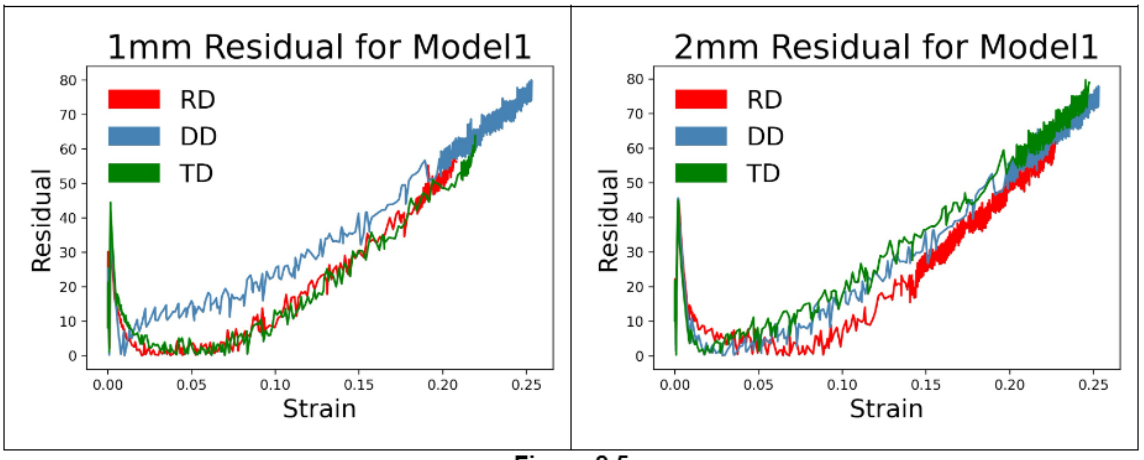

Figure 2.5

Therefore, in order to reduce the difference between the experimental data and the predicted data, the group hopes to adjust the Ludwik-Hollomon law behind, trying to reduce the residual to make the model more accurate.

3.2 Model 2 – Ludwigon Law

Although the Ludwik-Hollomon law describes the strain hardening behavior, the result does not seen as a properly model for prediction. Therefore, the Ludwigon equation is to use of modified Ludwik model:

$$\sigma_{true} = K_1 \varepsilon_p^{n_1} + \Delta \qquad where\ \Delta = exp(k_2 + n_2 \varepsilon_p)\ or \quad ln(\Delta) = K_2 + n_2 \varepsilon_p \tag{1.5}$$

Where $K_1 and\ n_1$ are the same in the Holleman equation respectively And K_2 and n_2 are additional constants. The correct term is for the deviation at low strain from the standard power law relationship for giving an explanation on this stress deviation appropriately.

K_1 : The material property constant called "strength coefficient"

$exp(K_2)$: The true yield stress in Ludwigon.

n_1 : The exponent termed the "strength harding component"

n_2 : The strain hardening exponent at low strain region, the slope of relationship of and true strain

Δ : The deviation parameter.

The Ludwik relation is convenient because it can be made linear by logarithmic transformation.

We take the RD of 1mm for example, in the right hand side of figure 2.6, we transfer true stress and strain into a log-log plot. In comparison with experimental data, we find that when true strain is small, there are some differences with computed data. When the true strain increases, it is obvious that the difference between experimental data and model data is gradually small.

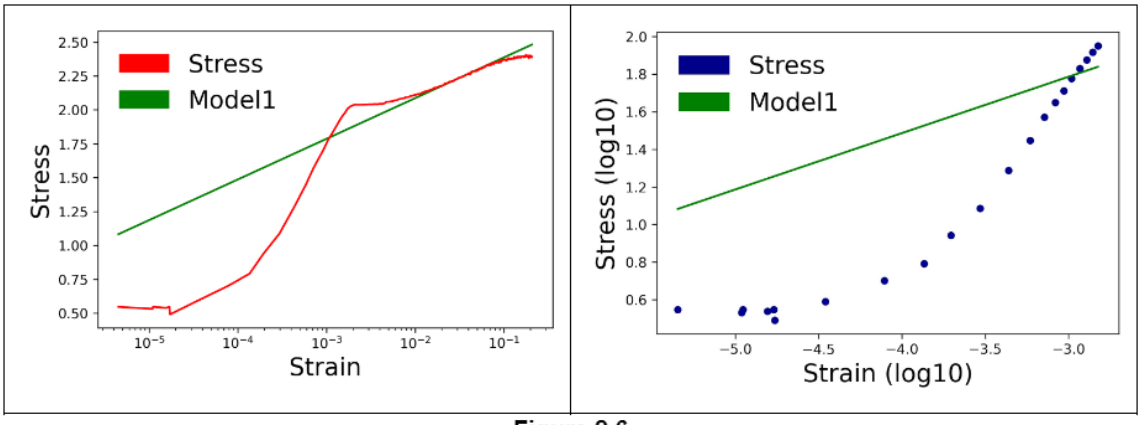

Figure 2.6

And this gap is defined in Model 2, and the difference between Model 2 and Ludwik-Hollomon law is also approximated by $\Delta = exp(k_2 + n_2 \varepsilon_p)\ or \quad ln(\Delta) = K_2 + n_2 \varepsilon_p$. Therefore, through the model, we can draw a comparison between the predicted map of 1mm and 2mm and the actual map, as shown in Figure 2.7.

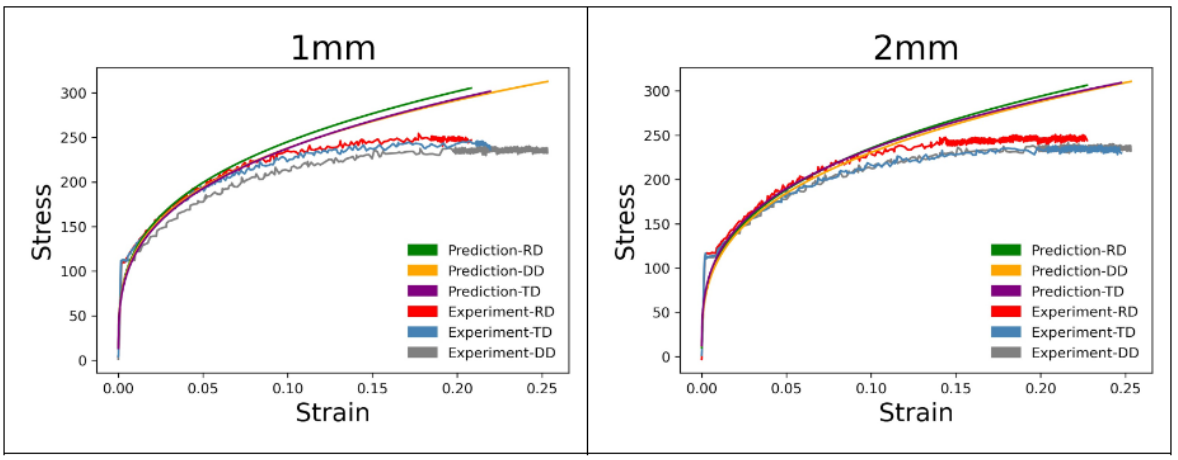

Figure 2.7

However, we found that the experimental data did not change much between Ludwik-Hollomon law and Ludwigon Law, the results were roughly the same as Ludwik-Hollomon law. The residual map is not particularly different from the residual map of Model1, as shown in Figure 2.8.

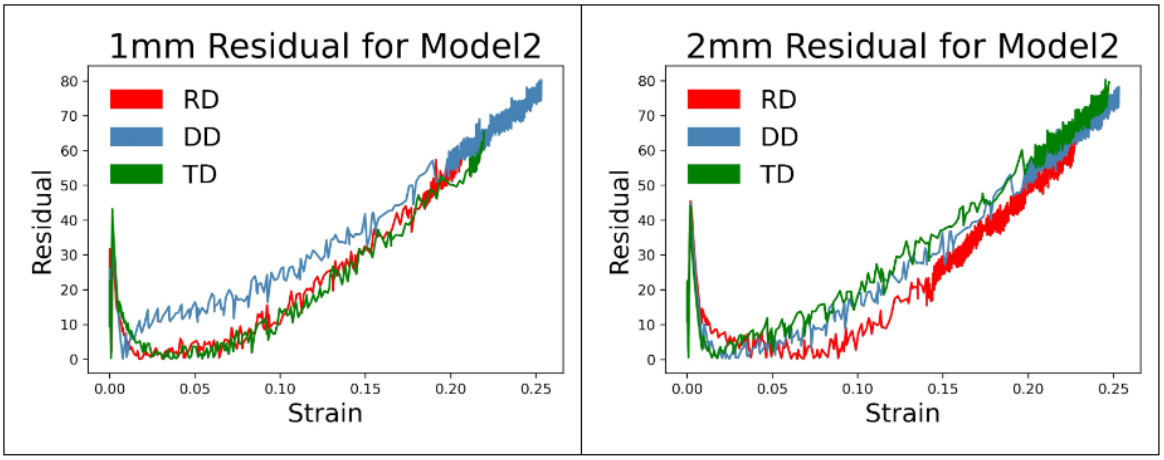

Figure 2.8

3.3 Model 3 – Voce constitutive model

$$\sigma = \sigma_0 + q(1 - exp(- b\varepsilon)) \quad (1.6)$$

Where,

σ_0 : The yeild stress

q, b: The material constants for Voce work hardening.

The material constants of Voce's constitutive model for AA5754-O are listed as following table:

Table 4 *Mechanical properties of the Voce strain hardening model for AA5754-O aluminum alloy*

σ0 (Mpa)	q	b
119.870	188.000	11.200000

*** E refers to Young's modulas , here we use E = 68 Gpa**

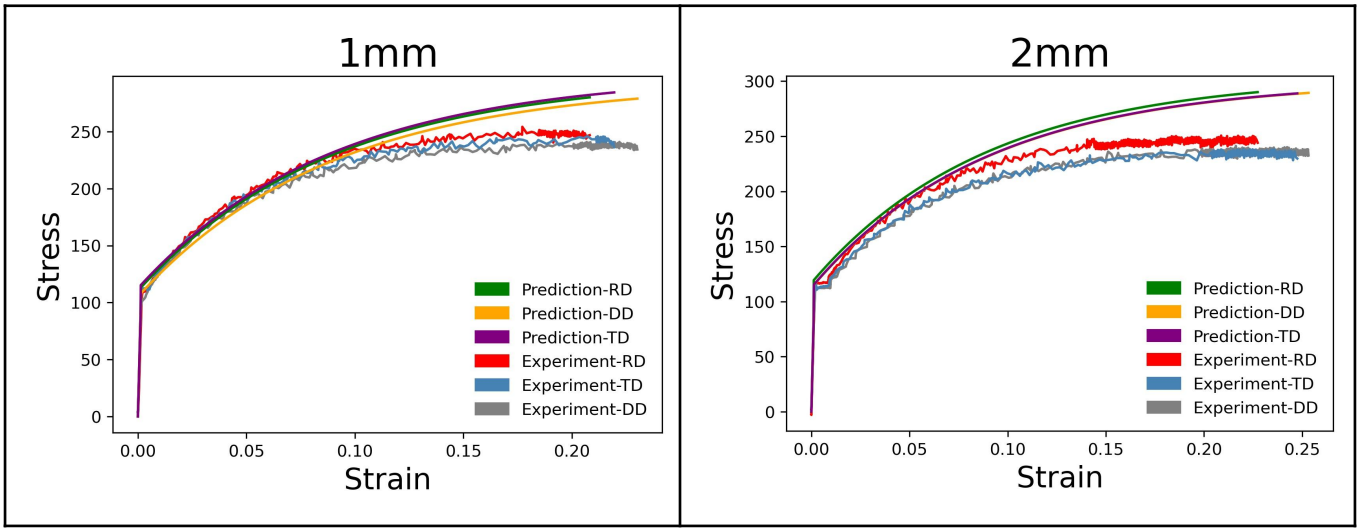

- Voce constitutive model overestimates the stress after necking point (ultimate tensile stress).

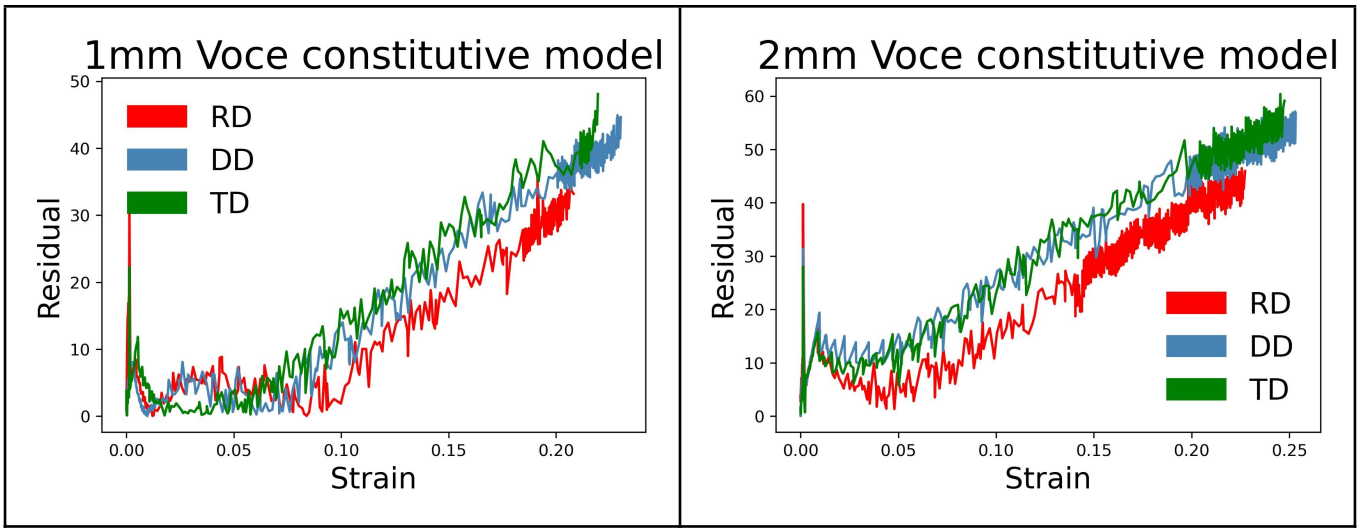

3.4 Model 4 – Modified Voce hardening model

$$\sigma = p - q \times exp(-b\varepsilon) + h\varepsilon \quad (1.7)$$

p, q, b, and h: The material constants for modified Voce hardening model.
The material constants of modified Voce hardening model for AA5754-O are listed as following table:

Table 5 *Mechanical properties of the modified Voce strain hardening model for AA5754-O aluminum alloy*

p	q	b	h
247.000	128.600	15.720000	242.000000

*** E refers to Young's modulas , here we use E = 68 Gpa**

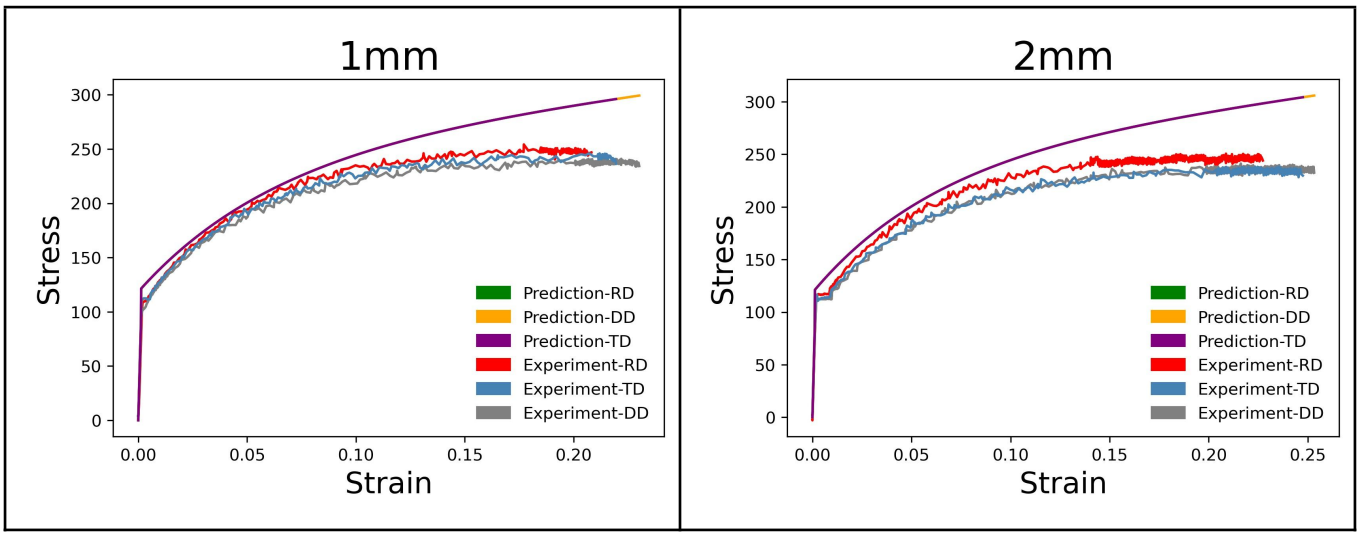

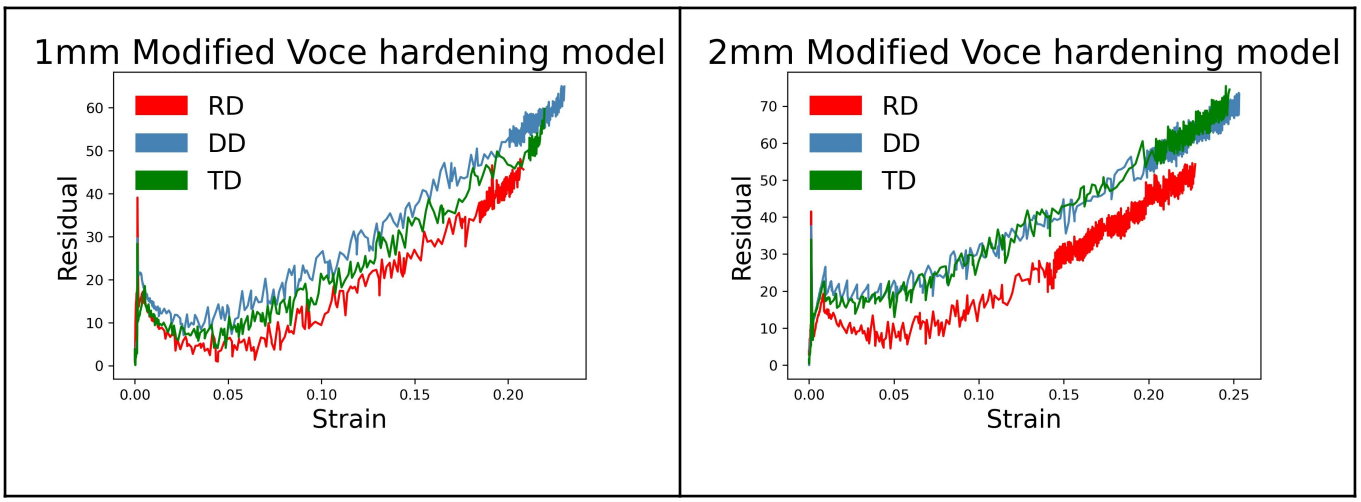

3.5 Model 5 – Swift model

$$\sigma = K(\varepsilon + \varepsilon_0)^n \tag{1.9}$$

Where,

K: The material property constant called “strength coefficient”

n: The exponent termed the “strength harding component”

ε_0: Yield strain

The material constants of Swift strain hardening model for AA5754-O are listed as following table:

Table 6 *Mechanical properties of the modified Voce strain hardening model for AA5754-O aluminum alloy*

K (MPa)	ε0	n
476.600	0.010	0.307300

*** E refers to Young's modulas , here we use E = 68 Gpa**

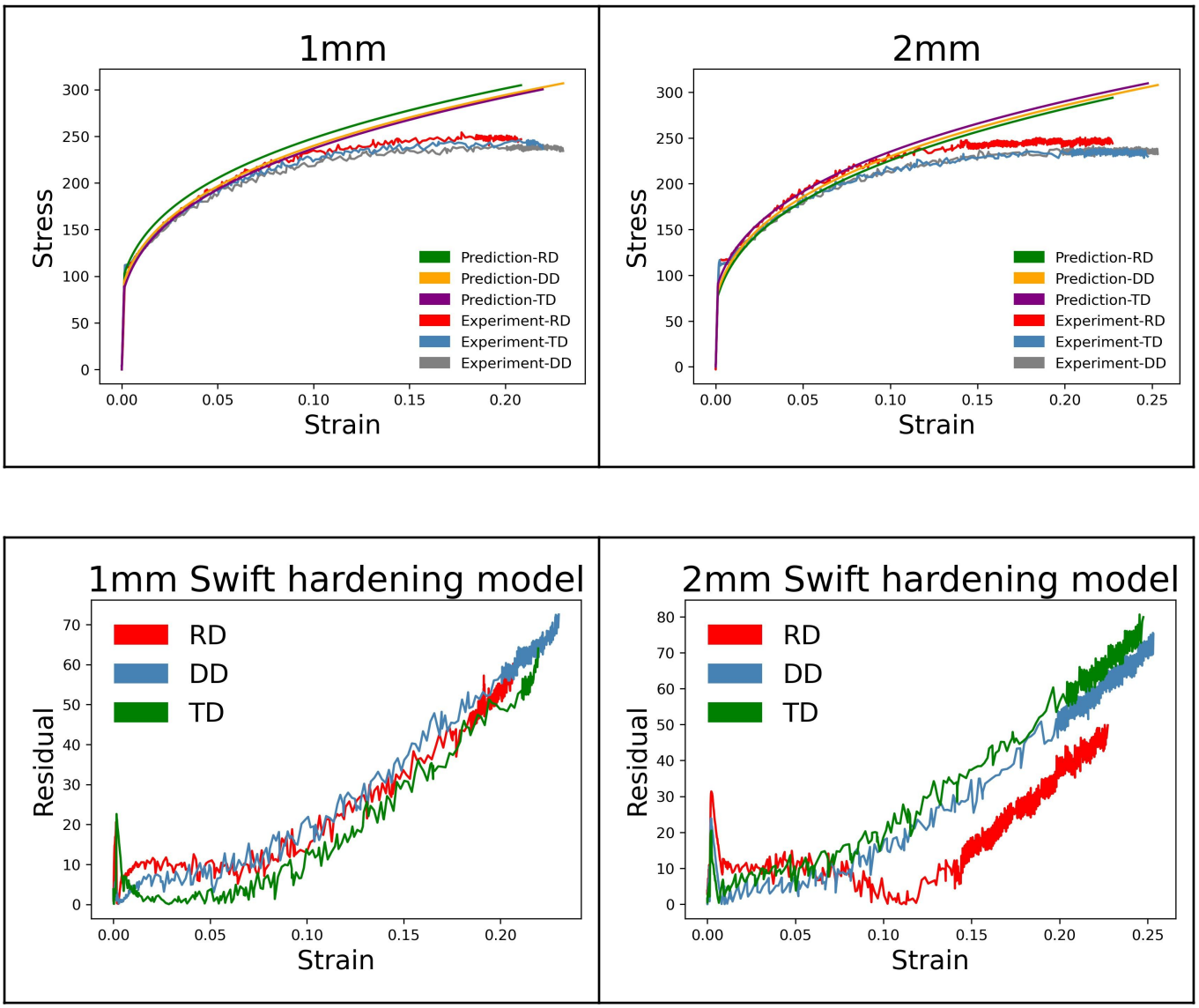

The Swift model fits the experiment data very well before the necking point (ultimate tensile stress), but it overestimates the stress when strain gets larger.

3.6 Model 6 – Kim-Tuan constitutive model

$$\sigma = \sigma_0 + K[1 - exp(-t\varepsilon)](\varepsilon + \varepsilon_0)^h \quad (1.8)$$

This model is the linear combination of the Swift model and Voce work hardening model.
Where,
K, t, and h: The material constants.

$$t = \frac{5}{\varepsilon^*}$$

$$h = \frac{\sigma^*}{\sigma^* - \sigma_0}\left(\varepsilon^* + \varepsilon_0\right)$$

$$K = \frac{\sigma^* - \sigma_0}{\left(\varepsilon^* + \varepsilon_0\right)^{\sigma^*(\varepsilon^* + \varepsilon_0)/(\sigma^* - \sigma_0)}}$$

The ε^* *and* σ^* referred to the strain and stress at the necking point (ultimate tensile strength).
The material constants of Kim-Tuan constitutive model for AA5754-O are listed as following table:

Table 7 *Mechanical properties of the Kim-Tuan strain hardening model for AA5754-O aluminum alloy*

σ0 (Mpa)	ε0	εs	k	a	h	t
119.870	0.010	0.220000	328.380000	1.426	0.772400	5.113000

*** E refers to Young's modulas , here we use E = 68 Gpa**

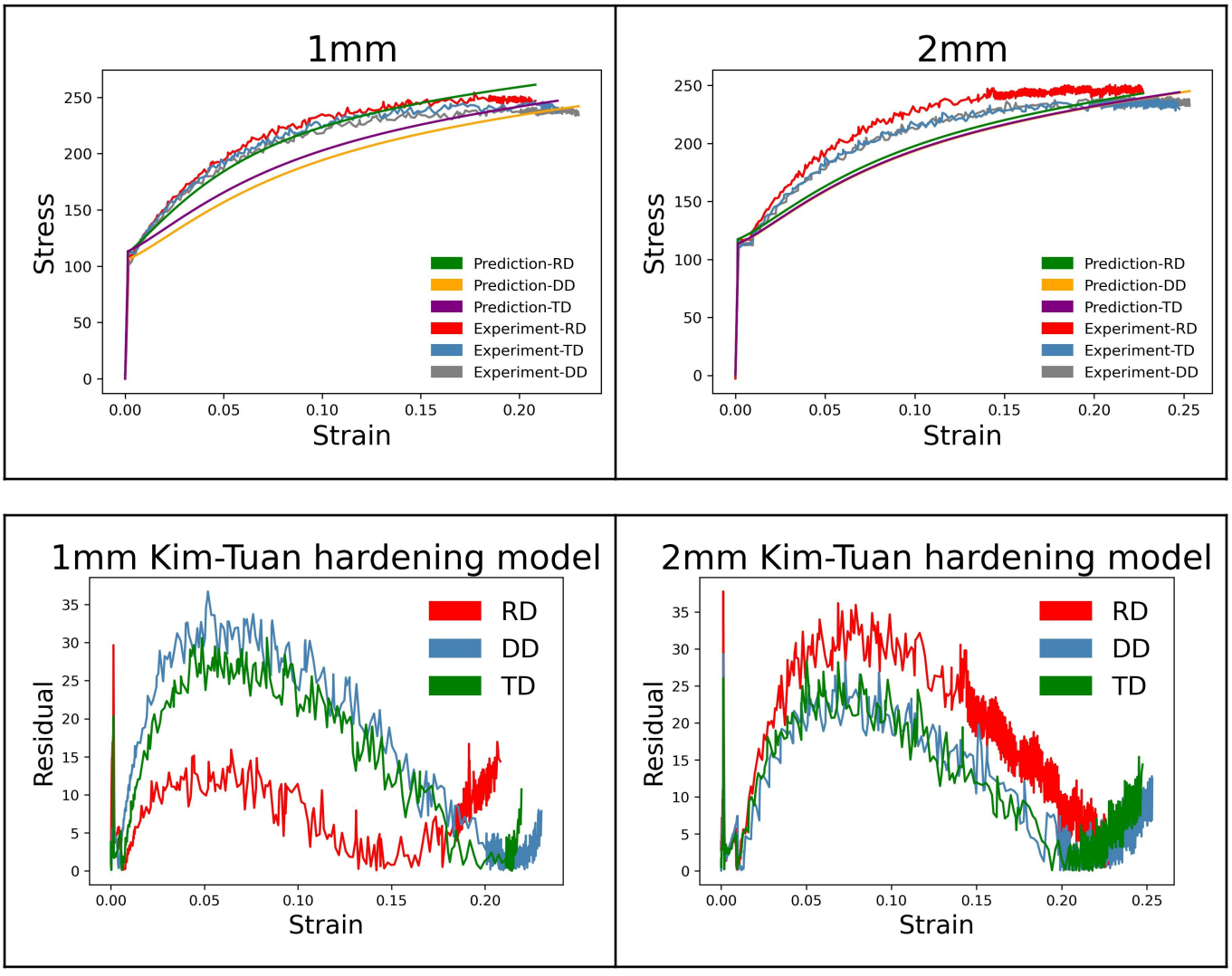

The Kim-Tuan constitutive model fits the experiment data well in general, and it can predict strain curve after necking, where the other models mentioned above do not perform well. However, the Kim-Tuan constitutive model underestimates the strain curve before necking but after yielding. Therefore, Kim-Tuan constitutive model is suitable for post-necking prediction.

4. Conclusion

4.1 Model Evaluation

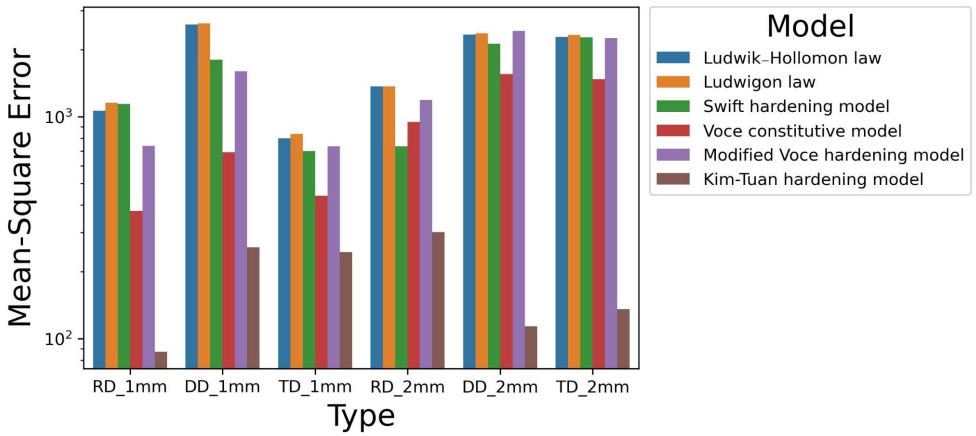

In the Mean-square error (MSE) histogram, it can be seen that the Kim-Tuan hardening model is the model with the lowest MSE among them. Therefore we decided that the Kim-Tuan hardening model is the best model to fit our experimental data.

4.2 Pick 3 out of 5 categories

In this part, we first describe briefly about the rolling process. And chose 3 categories (deformation, surface and heat transfer) which we learned in the class about our project.

4.2.1 Deformation

a) Rolling process

Tensile test can be used to obtain not only the relationship between the strain and stress of the material but also the ductility of the material, and to predict ductile fracture is important in rolling processes, especially in cold rolling processes. In rolling processes, the material undergoes plastic deformation before fracture, but we must know how far the material can be deformed and not cause any fracture. To know the ductility of the material, we can do a tensile test.

b) Sheet forming

A critical problem in sheet forming is how to avoid fracturing, and tensile test can predict fracture during sheet forming. Also, we can get a better understanding of the material used for the sheet forming process. For example, we are able to know the material's stress-strain relationship so as to know how much the material can be deformed and how much stress might make material necking or cracking.

c) Extrusion

By doing tensile tests, we can determine the extrusion force and prevent the stressed material from fracturing during the extrusion process. Also, tensile tests allow us to interpret the changes of mechanical properties during the process.

4.2.2 Surface

a) Cold-drawing

The fracture surfaces of tensile tests can be used to study the cold-drawing fracture behavior. The fracture surfaces obtained by tensile test can be analyzed by scanning electron microscopy (SEM), and then we

can get an understanding of the relationship between fracture surface and applied stress. For example, the fracture surface might be smoother when applying stress at a slower rate, on the other hand, the fracture surface might be rougher when increasing the stress at a higher rate.

4.2.3 Heat sources

a) Hot working

Manufacturing in high temperatures will have thermal stress which will cause failure, and there is a method called Hot tensile test to evaluate the material properties strength at certain high temperatures. Many manufacturing processes such as hot rolling, hot drawing, and extrusion can benefit from knowing of both mechanical and thermal properties.

5. Reference

[1] CEN, Workshop Agreement, CWA 15627:2006 E "Small Punch Test Method for Metallic Materials, 2006.

[2] García, T. E., Rodríguez, C., Belzunce, F. J., & Suárez, C. (2014). Estimation of the mechanical properties of metallic materials by means of the small punch test. Journal of alloys and compounds, 582, 708-717.

[3] Yang, S. S., Ling, X., Qian, Y., & Ma, R. B. (2015). Yield strength analysis by small punch test using inverse finite element method. Procedia Engineering, 130, 1039-1045.

[4] M. Abendroth, M. Kuna, Determination of ductile material properties by means of the small punch test and neural networks, Adv. Eng. Mater. 6 (7) (2004) 536–540.

[5] Li, K., Peng, J., & Zhou, C. (2018). Construction of whole stress-strain curve by small punch test and inverse finite element. Results in Physics, 11, 440-448.

[6] Holmberg, S., Enquist, B., & Thilderkvist, P. (2004). Evaluation of sheet metal formability by tensile tests. *Journal of materials processing technology*, *145*(1), 72-83.

[7] Tiernan, P., & O'Connor, G. (2018). Design, manufacture and test of a high temperature tensile and compression testing device. *Procedia Manufacturing*, *17*, 672-679.

[8] Sojodi, S., Basti, A., Falahatgar, S. R., & Nasiri, S. M. M. (2021). Investigation on the forming limit diagram of AA5754-O alloy by considering strain hardening model, strain path, and through-thickness normal stress. *The International Journal of Advanced Manufacturing Technology*, *113*(9), 2495-2511.

[9] Wang H, Wan M, Yan Y (2012) Effect of flow stress−strain relation on forming limit of 5754O aluminum alloy. Trans Nonferrous Met Soc China 22:2370–2378

[10] Hu Q, Li X, Chen J (2019) Forming limit evaluation by considering through-thickness normal stress: theory and modeling. Int J Mech Sci 155:187–196

[11] Kim YS, Lee BH, Yang SH (2018) Prediction of forming limit curve for pure titanium sheet. Trans. Nonferrous Met Soc China 28:319–327

[12]Simmons, J. (1997). Strain hardening and plastic flow properties of nitrogen-alloyed Fe-17Cr-(8–10)Mn-5Ni austenitic stainless steels. Acta Materialia, 45(6), 2467–2475.

[13]Kim, J.-H. ., Serpantié, A., Barlat, F., Pierron, F., & Lee, M.-G. . (2013). Characterization of the post-necking strain hardening behavior using the virtual fields method. International Journal of Solids and Structures, 50(24), 3829–3842.